Atmos. Chem. Phys. Discuss., https://doi.org/10.5194/acp-2017-506
Manuscript under review for journal Atmos. Chem. Phys.
Discussion started: 22 June 2017

Atmospheric Chemistry and Physics Discussions

The Effects of El Niño-South Oscillation on the Winter Haze Pollution of China

Shuyun Zhao[1,2], Hua Zhang[1,2], Bing Xie[1,2]

[1]Laboratory for Climate Studies, National Climate Center, China Meteorological Administration, Beijing, China
[2]Collaborative Innovation Center on Forecast and Evaluation of Meteorological Disasters, Nanjing University of Information Science & Technology, Nanjing, China

Correspondence to: Hua Zhang (huazhang@cma.cn)

Abstract. It is reported in previous studies that El Niño-South Oscillation (ENSO) influences not only the summer monsoon, but also the winter monsoon over East Asia. This contains some clues that ENSO may affect the winter haze pollution of China, which has become a serious problem in recent decades, through influencing the winter climate of East Asia. In this work, we explore the effects of ENSO on the winter (from December to February) haze pollution of China statistically and numerically. Statistical results reveal that the haze days of southern China tend to be less (more) than normal in El Niño (La Niña) winter; whereas the winter haze days of northern and eastern China have no significant relationship with ENSO. Results from numerical simulations show that under the emission level of aerosols for the year 2010, the winter-average atmospheric contents of anthropogenic aerosols over southern China are generally more (less) than normal in El Niño (La Niña) winter. It is because that the transports of aerosols from South and Southeast Asia to southern China are enhanced (weakened), which mask the better (worse) scavenging conditions for aerosols in El Niño (La Niña) winter. The probability density function (PDF) of the simulated daily surface concentrations of aerosols over southern China indicates that the region tends to have less clean and moderate (heavy) haze days, but more heavy (moderate) haze days in El Niño (La Niña) winter.

1 Introduction

Haze pollution, especially in winter, has become a very serious problem for China in recent decades (Ding and Liu, 2014; Tao et al., 2016). For example, in January 2013, most parts of central and eastern China experienced an extremely heavy and persistent haze pollution (Tao et al., 2014; Mu and Zhang, 2014; Zhang et al., 2014; Wang et al., 2014a; b; Zou et al., 2017). In the last decade, haze pollution in winter has received wide concerns from the scientific community, the government of China,

and the public.

Haze pollution is a phenomenon mainly caused by human-emitted pollutants under stagnant meteorological conditions. Increasing anthropogenic emissions of aerosols and their precursors in recent decades are the main reasons for the worsening air qualities in China (Cao et al., 2007; Zhang et al., 2012; Zhu et al., 2012). In addition to the increase in anthropogenic emissions of aerosols and their precursors, climate changes caused by anthropogenic and/or natural forcings also exert great influences on the haze pollution in China, especially through changing the strength of East Asian Monsoon (Zhang et al., 2010; 2014; Liu et al., 2011; Yan et al., 2011; Chin, 2012; Zhu et al., 2012; Mu and Zhang, 2014; Chen and Wang, 2015; Li et al., 2016a; b; Cai et al., 2017). Studies generally showed that the wintertime haze days across central and eastern China had a close negative relationship with the strength of the East Asian Winter Monsoon (EAWM) (Zhang et al., 2014; Mu and Zhang, 2014; Chen and Wang et al., 2015; Li et al., 2016a; Cai et al., 2017). In summer, the increase in surface aerosol concentration and optical depth over eastern and northern China always correlates with the weakening of East Asian Summer Monsoon (EASM) (Zhang et al., 2010; Yan et al., 2011; Zhu et al., 2012).

Wang et al. (2015) and Zou et al. (2017) revealed that the increasing winter haze pollution in eastern China in recent years was related to the decreasing Arctic sea ice in preceding autumn. Many studies suggested that under global warming, the future climate would be more stagnant and the weather conditions conducive to severe haze in eastern China would be more frequent (Jacob and Winner, 2009; Wang et al., 2015; Cai et al., 2017). But Jacob and Winner (2009) also pointed out that the effects of future climate change on particulate matter (PM) were complicate, as the projection of precipitation, wildfires, atmospheric chemistry, and natural emissions of aerosols by models were still in need of improvement.

ENSO is the dominant changing mode of the tropical sea surface temperature (SST) on interannual scale (Rasmusson and Carpenter, 1982), of which the climatic effects are global (Bjerknes, 1972; Huang and Wu, 1989; Zhang et al., 1999; Lau and Nath, 2003; Zhai et al., 2016, etc.). ENSO not only influences the EASM (Chang et al., 2000; Li et al., 2007; Zhao et al., 2017, etc.), but also influences the EAWM, especially over low latitudes (Chen et al., 2013; He and Wang, 2013; Kim et al., 2016, etc.), which means that ENSO may affect the winter haze pollution of China through its influences on EAWM. Gao and Li (2015) revealed statistically that El Niño (La Niña) events were more likely to bring more (less) haze days in eastern China. Feng et al. (2017) simulated the influences of the 1994/1995 El Niño Modoki event on the aerosol concentrations over southern

China, and found that aerosol concentrations increased during the mature phase (in boreal winter) of the event. However, studies investigating the effects of ENSO on the winter haze pollution of China are still not enough nor comprehensive. ENSO is a recurring climate pattern, and many climate centers of the world monitor it systematically and use it in climate prediction extensively. Therefore, exploring the effects of ENSO on the winter haze pollution in China may provide useful information in the prediction of haze for the country.

This work explores the effects of ENSO on the winter haze pollution of China statistically and numerically. The article is organized as follows: methodology is given in section 2, including data and model introduction; results including statistical and model results, are presented in section 3, followed by conclusions and discussions in section 4.

2 Methodology

2.1 Data used in statistical analysis

We firstly analyze the relationship between the winter haze days of China and global SST in section 3. The monthly haze days from the data set for haze project version 1.0 of the National Meteorological Information Center, China Meteorological Administration (CMA) are used. The CMA defines haze using visibility (<10 km) and relative humidity (<80%) (Tao et al., 2014). The time-span of the data set is January 1954 ~ July 2014, but only the data after 1960 are actually used in this study, as the data set has steadily included more than 2000 stations since 1960. A merged monthly SST data (Hurrell, et al., 2008) formed by the SST data of the Hadley Centre and the National Oceanic and Atmospheric Administration (NOAA) is used in the correlation analysis. The SST data together with a merged sea ice (SI) data of the same sources are used in the following numerical simulation. The SST and SI data are both from 1870 to 2012, with a horizontal resolution of 1°×1°.

2.2 Model description and experimental set-up

The aerosol-climate coupled model BCC_AGCM2.0_CUACE/Aero (Zhang et al., 2012) of the National Climate Center (NCC), CMA, is used in the numerical study of the effects of ENSO on the atmospheric contents of aerosols. The coupled model composes of the NCC/CMA climate model (BCC_AGCM2.0, Wu et al., 2010) and the CMA Unified Atmospheric Chemistry Environment/Aerosol model (CUACE/Aero, Gong et al., 2002, 2003). The coupled model employs a horizontal T42 spectral resolution (about 2.8°×2.8°) and a hybrid vertical coordinate with 26 levels, the top of which is located at about 2.9 hPa. Five types of aerosols (including their emissions, gaseous chemistry, transports, coagulations, and removals): sulfate (SF), black

carbon (BC), organic carbon (OC), dust, and sea salt are considered in the model. The emissions of the first three types of aerosols and/or their precursors are prescribed, and the last two types of aerosols are emitted online (Gong et al., 2002). The particle radii of each type of aerosol are divided into 12 size bins from 0.005 to 20.48 μm. All types of aerosols are assumed to be externally mixed with each other. Sulfate, organic carbon, and sea salt are assumed to be hygroscopic, and the other two types of aerosols are assumed to be non-hygroscopic. The coupled model has been introduced, evaluated, and used in many studies of the radiative forcing and climatic effects of aerosols (e.g., Wang et al., 2015; Zhao et al., 2014; Zhang et al., 2016).

Three groups of experiments are conducted (Table 1), named CLI, EL, and LA, with each group including 20 members by altering initial conditions. To get different initial conditions, a preparation experiment is run firstly with the model's default setting (Zhao et al., 2014). Three types of files (initial, restart, and history files) of the preparation experiment are output, and the output frequency is set to daily. 20 initial files output from the preparation experiment are then used as the different initial conditions for different ensemble members. The group of CLI uses the climatological-mean (from 1981 to 2010) monthly SST and SI, which have been introduced in the section 2.1 but interpolated to the model's resolution, as boundary conditions. In the groups of EL and LA, the climatological-mean monthly SST is superposed by El Niño and La Niña SST perturbations, respectively, and the SI is identical to that in CLI. The El Niño and La Niña SST perturbations are obtained by scaling a typical ENSO mode (Figure 1a) with the average monthly Niño3.4 indices of 21 El Niño and 18 La Niña events (selected from 1951 to 2015, Figure 1b), respectively. The Niño3.4 indices from January 1951 to date can be downloaded from the website of NCC/CMA (cmdp.ncc-cma.net/download/Monitoring/Index/M_Oce_Er.txt). The typical ENSO mode is obtained through the regression between the monthly Niño3.4 index and the SST field after removing their linear trends. The running period of the group of CLI is from October to the next August, to testify if the model can capture the general features of the circulations of the East Asian winter and summer monsoons. In the testifying process, geopotential height and wind from the National Centers for Environmental Prediction (NCEP) reanalysis data are used. Whereas the running periods of EL and LA are both from October to the next February. The results in boreal winter (from December to February) of the three groups are used in analysis, allowing prior two months for the atmosphere to response to SST perturbations.

The emission data of SF, BC, OC, and/or their precursors used in all experiments are from the Representative Concentration Pathway 4.5 (RCP 4.5) of the Intergovernmental Panel on Climate Change (IPCC) for the year of 2010. In this study, only the

changes in the atmospheric contents of SF, BC, and OC caused by different SST perturbations are analyzed, as the three types of aerosols are mainly emitted by anthropogenic activities and important components of haze pollutants.

3 Results

3.1 Statistical results

In this part, we firstly present the geographical distribution of the winter-average haze days in mainland China over the past ~50 years and since 2000. Then, three typical polluted regions are selected, and the correlations between the winter haze days of each selected region and the global SST are analyzed.

It is seen from Figure 2a that Beijing, the southwest part of Hebei, the central and south parts of Shanxi, the central part of Shaanxi, and the north part of Henan province suffered haze pollution more frequently than elsewhere in China during the winters of 1960−2013. Besides the above areas, stations with more than 5 winter-average monthly haze days during 1960−2013 also distributed densely in the provinces of Hubei, Hunan, Jiangxi, Zhejiang, Guangxi and Guangdong. Compared with 1960−2013, winter haze pollution in mainland China generally became more frequent in the winters during 2000−2013 (Figure 2b). For example, in the provinces of Jiangsu, Zhejiang, and Guangdong, stations with 5~10 and 10~20 winter-average monthly haze days during 2000−2013 were much more than that during 1960−2013. At some stations of Shanxi province, the winter-average monthly haze days during 2000−2013 were more than 20 (Figure 2b), which was not seen in Figure 2a; In 2013, the winter-average monthly haze days was horribly 29 at Linfen station in Shanxi province.

Three representative regions: JJJ (Beijing, Tianjin, and Hebei province; accounting for 179 stations), JZH (Jiangsu and Zhejiang provinces, and Shanghai; accounting for 164 stations), and GG (Guangdong and Guangxi provinces; accounting for 178 stations) are selected to represent northern, eastern, and southern China, respectively. It is seen from Figure 3 that the winter-average monthly haze days of JJJ, JZH, and GG were generally less than 3 before the year of 2000, with a small peak around 1980 in JJJ and JZH. After the year of 2000, the winter-average monthly haze days over the three regions grew dramatically, especially over JZH and GG. The winter-average monthly haze days of JJJ increased much later than the other two regions after the year of 2000. Actually, the winter-average monthly haze days in JJJ were relative few until 2012, which was consistent with the result of Chen and Wang (2015).

Considering that the increases in winter-average monthly haze days over JZH and GG increased too abruptly after the year of

2010, especially in 2013, only the winter-average monthly haze days of the three regions from 1960 to 2010 are used in analyzing their relationships with winter SST, after applying a linear-trend removing and a 2-8 years band-pass filtering to both the data of haze days and SST. It is seen from Figure 4 that only the winter haze days of GG have significant negative relationships with the equatorial SST over central and eastern Pacific and central Indian Ocean, and positive relationships with the equatorial SST over western Pacific. The geographical distribution of the correlation coefficients between GG winter haze days and SST is generally a reverse of the typical ENSO mode shown in Figure 1a, indicating that southern China tends to suffer more (less) haze days than normal in La Niña (El Niño) winter. The winter haze days of JJJ and JZH have no significant relationships with equatorial SST, indicating that ENSO does not influence the winter haze days of northern or eastern China significantly. It's probably because that as a tropic phenomenon, ENSO affects the climate over southern China more directly than over other regions of China, especially in winter. Zou et al. (2017) linked the extreme winter haze over East China Plains (112º~122ºE, 30º~41ºN, including JJJ and most parts of JZH) to Arctic sea ice loss in the preceding autumn and extensive Eurasia snow fall in early winter. Gao and Li (2015) found that the winter haze days of eastern China had positive relationship with the SST over eastern equatorial Pacific. But the "eastern China" in Gao and Li (2015) included most regions between the Yangtze and Yellow rivers east of 105ºE, which was much larger than the representative region of eastern China in this work, and more south and west than the concerned region in Zou et al. (2017).

3.2 Model results

3.2.1 Winter and summer circulations, and the atmospheric contents of aerosols

First of all, the simulated winter and summer circulations over East Asia in the group of CLI are testified by comparing with NCEP reanalysis data (Figure 5). The model can capture the general features of the winter and summer circulations over East Asia. For example, in winter, the deepening of East Asian Trough (EAT), the overwhelming of northwesterly over east parts of China, and the strengthening of the easterly north of the equator are all depicted by model results (Figure 5a); In summer, the northward shift of Western Pacific Subtropical High (WPSH), and the strengthening of the cross-equatorial westerly over Indian Ocean and Maritime Continent are generally captured by the model (Figure 5b). But the simulated EAT in winter by the model is weaker and narrower, and locates more west than NCEP reanalysis data. In summer, the simulated WPSH is weaker and locates more east than NCEP reanalysis data. It seems that the simulated cross-equatorial flow is stronger than

reanalysis data both in winter and summer, which is probably the reason for the weakness of the simulated EAT in winter and WPSH in summer. In the model results of the group of CLI, the stronger cross-equatorial westerly over Indian Ocean and Maritime Continent obstructs the westward stretch of the WPSH in summer, resulting in positive precipitation biases over South Asia and Southeast Asia, and negative precipitation biases over Southern China (Zhao et al., 2014).

The simulated winter surface concentrations (CONCsur) of aerosols and aerosol loadings in the group of CLI (Figure 6) show that central and eastern China (about east of 105ºE) are the most haze polluted regions of the country, in line with the observational distribution of winter haze days shown in Figure 2. The maximum of the winter CONCsur of aerosols centers in Henan province, and is about 20 μg m^{-3}. Comparing with other observational studies (e.g., Cao et al., 2007; Zhang and Cao, 2015; Cai et al., 2017), the simulated CONCsur of aerosols shown in Figure 6a are underestimated by about 1~2 orders of magnitude. It should be illustrated that the aerosol CONCsur in this study are the aerosol concentrations at the lowest level of the model. As has been introduced in section 2.2, the model used in this study has 26 levels in the vertical hybrid σ-pressure axis, and the mid height of the lowest level is about 50 ~ 70 meters above the surface in China (not shown). Therefore, the aerosol concentrations at the lowest level of the model actually reflect the mean of the aerosol concentrations from the surface to a height of about 100 ~ 140 meters (or maybe even higher) above the surface. This certainly brings about underestimations as to aerosol CONCsur. Another reason for the underestimation is that we exclude all nature-emitted aerosols, in order to focus our attentions on haze, as another meteorological disaster occurring frequently in late winter and spring over northern China – sandstorm – has quite different weather conditions with haze. The exclusion of nature-emitted aerosols (mainly dust aerosol) is also the reason why the northwestern China is much cleaner than it is expected to be.

The maximum of the simulated winter aerosol loadings in China is 21 ~ 25 mg m^{-2}, and heavy aerosol loadings (≥18 mg m^{-2}) in China locate east of 105°E, and between the Yellow and Yangtze rivers (Figure 6b). The median of 10 models that participate in Aerosol Comparisons between Observations and Models (AeroCom, http://aerocom.met.no/cgi-bin/aerocom/surfobs_annualrs.pl) shows that the maximums of the loadings of SF, BC, and OC in January 2000 in China are 15 ~ 30, 2.5 ~ 5, and more than 10 mg m^{-2}, respectively. The model used in this study is also a member of AeroCom. Zhao et

al. (2014) have compared the simulated loadings of five kinds of aerosols (SF, BC, OC, sea salt, and dust) by the model with AeroCom median, and found that the model generally simulated the distributions and magnitudes of aerosol loadings well, though with some underestimation in BC and OC.

3.2.2 The effects of ENSO on winter circulation and precipitation

The effects of ENSO on winter circulation and precipitation over East Asia are discussed firstly, as these meteorological fields determine the transports, diffusions, removals, and consequently the atmospheric contents of aerosols.

Two important features are apparent in the winter anomalous circulation field caused by El Niño (Figure 7a). Firstly, negative and positive anomalous geopotential heights at 500 hPa are seen near Ural Mountains and Lake Baikal, respectively, which indicates the weakness of EAWM. Studies have found that EAWM tended to be weak during El Niño winter (Chen et al., 2000; Huang et al., 2012; Wang and Chen, 2014). Secondly, an anomalous anticyclone at 850 hPa is seen over western North Pacific. Wang et al. (2000) found that the anomalous anticyclone over western North Pacific formed in the boreal autumn of a developing El Niño, attained its peak in winter, and persisted into the following spring and early summer. The appearance of the anomalous western North Pacific anticyclone is an important sign of the response of EAWM circulation to El Niño. It is expected that the anomalous southwesterly in the northwest of the anticyclone brings more water vapor and also more aerosols to southern China, as Indo-China Peninsula and South Asia are both areas with heavy aerosol loadings (Figure 6b). The anomalous geopotential height at 500 hPa caused by La Niña are positive and negative near Ural Mountains and Lake Baikal, respectively, and an anomalous cyclone is caused by La Niña over western North Pacific (Figure 7b).

Corresponding to the anomalous anticyclone at 850 hPa over western North Pacific caused by El Niño, winter precipitation decreases over Indo-China Peninsula and western North Pacific, and increases over southern China (Figure 8a). In contrast, precipitation increases over Indo-China Peninsula and western North Pacific, and decreases over southern China during La Niña winter (Figure 8b). The decrease in winter precipitation over southern China caused by La Niña is the reason for the more-than-normal haze days in GG during La Niña winter indicated in Figure 4c, as less precipitation means slower cleaning particles out of the atmosphere. Another reason probably cannot be neglected that drier conditions over southern China during La Niña winter can avoid mistaking haze to fog days.

Atmos. Chem. Phys. Discuss., https://doi.org/10.5194/acp-2017-506
Manuscript under review for journal Atmos. Chem. Phys.
Discussion started: 22 June 2017

Atmospheric Chemistry and Physics Discussions

3.2.3 The effects of ENSO on winter atmospheric contents of aerosols

In this section, the changes in the winter aerosol CONCsur and loadings over China caused by ENSO are presented, and then the mechanism how ENSO affects the winter atmospheric contents of aerosols is analyzed from the perspective of wet and dry depositions and interregional transports of aerosols.

It is seen from Figure 9a that the winter CONCsur of aerosols are decreased by El Niño over northeastern China, parts of Shandong and Anhui provinces, and most parts of JZH; but increased by El Niño over southwestern Shaanxi province, Ningxia, eastern Gansu and Sichuan provinces, and most parts of Yunnan province. The winter aerosol CONCsur are decreased by La Niña over northeastern China, eastern Inner Mongolia, the north part of JJJ, and most areas south of the Yangtze river; but increased by La Niña over Shaanxi province, Ningxia, most parts of Shanxi and Henan provinces, southwestern Hebei province, northern Chongqing and Hubei provinces, and eastern Sichuan and Gansu provinces (Figure 9b). It is found from Figure 9c that winter aerosol loadings are increased by El Niño over most areas east of 105ºE and south of 40ºN, and decreased over northeastern China and the north part of JJJ. From Figure 9d, it is seen that the anomalous winter aerosol loadings caused by La Niña present a meridional "- + -" pattern over the areas east of 105ºE.

Comparing the left and right panels of Figure 9, it is easily found that the geographical distributions of the anomalous winter atmospheric contents of aerosols caused by El Niño and La Niña are not quite different with each other over the areas north of the Yangtze river. This is because that the responses of winter circulations to El Niño and La Niña are not opposite with each other over higher latitudes, e.g., the EAT is both strengthened by El Niño and La Niña, leading northerly wind to the northeast part of China (Figure 7). And this is also to some extent in line with the results in section 3.1 that the winter haze days over northern and eastern China have no significant relationship with ENSO. However, over southern China, the anomalous atmospheric contents of aerosols caused by El Niño and La Niña are quite opposite to each other, with increased atmospheric contents of aerosols caused by El Niño and decreased atmospheric contents of aerosols caused by La Niña, which is generally in line with the simulation result of Feng et al. (2017). Therefore, in the following analysis, we focus on the mechanism how ENSO affects the winter atmospheric contents of aerosols over southern China.

It has been discussed in section 3.1 that the haze days over southern China tended to be less (more) than normal in El Niño (La Niña) winter, which is to some extent contradictory to the increase (decrease) in winter atmospheric contents of aerosols

over southern China caused by El Niño (La Niña). In the following of this section, we firstly explore the reasons for the increase (decrease) in winter atmospheric contents of aerosols caused by El Niño (La Niña) over southern China. Then, we try to explain why the changes in winter haze days and winter-average atmospheric contents of aerosols caused by ENSO over southern China are not consistent with each other.

As the emissions of aerosols are kept the same in all experiments (section 2.2), the removals of aerosols from the atmosphere, especially through wet deposition, can affect the atmospheric contents of aerosols greatly (Zhang et al., 2016). It is found that the winter-average wet depositions of aerosols over southern China are increased (decreased) by El Niño (La Niña) (Figure 10a and b), corresponding to the changes in winter precipitation (Figure 8). The winter-average dry depositions of aerosols are decreased both by El Niño and La Niña over southern China (Figure 10c and d), but with much smaller amplitude of variation comparing with wet depositions. Comparing Figure 9 and 10, it seems that the changes in winter-average depositions of aerosols are the results rather than the reasons of the changes in the winter atmospheric contents of aerosols over southern China.

Besides local emissions and removals, the interregional transports of aerosols can also influence the atmospheric contents of aerosols over a specific region. It was mentioned in Zhang et al. (2016) that South and Southeast Asia had become the important source areas of anthropogenic aerosols in 2010, which was also seen in the simulated aerosol CONCsur and loadings over these regions shown in Figure 6. A low-level anomalous anticyclone (cyclone) is caused by El Niño (La Niña) over western North Pacific in winter (Figure 7). The southwesterly (northeasterly) at the northwest of the anomalous anticyclone (cyclone) leads to an enhanced (weakened) the transports of aerosols from South and Southeast Asia to southern China in El Niño (La Niña) winter (Figure 11). As the changes in the winter atmospheric contents of aerosols over southern China caused by ENSO cannot be explained by local emissions or removals, it seems can only be attributed to the changes in the transports of aerosols from South and Southeast Asia to southern China. Zhu et al. (2012) has also pointed out that in determining aerosol concentrations, the changes in monsoon circulation are more dominant than that in precipitation (or wet deposition of particles) in East Asia.

It has been revealed statistically in Figure 4c that southern China tended to suffer more (less) haze days than normal in La Niña (El Niño) winter, which was also reflected in two years near 2010 (in numerical simulation, the aerosol emissions for

2010 were used), e.g., a peak of winter haze days over GG appears in 2007 (with a La Niña winter), whereas a trough appears in 2009 (with an El Niño winter) (Figure 3). However, numerical results show that La Niña (El Niño) causes a decrease (increase) in the winter-average atmospheric contents of aerosols over southern China (Figure 9). Is it possible for southern China to have more (less) haze days but less (more) atmospheric contents of aerosols than normal in La Niña (El Niño) winter? To answer this question, the probability distribution function (PDF) of the simulated winter daily aerosol CONCsur averaged over southern China (21°N-27°N, 104°E-118°E) in winter is plotted in Figure 12. It has been illustrated in section 3.2.1 that the simulated aerosol CONCsur in this study were smaller than observational studies by 1~2 orders of magnitude. Therefore, for calibration, the simulated daily aerosol CONCsur in winter over southern China are amplified by 10 times before calculating PDF.

It is seen from Figure 12 that the PDF of the simulated winter daily aerosol CONCsur over southern China is a little right-skewed in the group of CLI, reaching peak at around 65 μg m^{-3}. The PDF of the simulated winter daily aerosol CONCsur over southern China in the group of LA is larger than that in CLI in the range of 45~85 μg m^{-3}, and smaller than that in CLI out of the range. The PDF of the simulated winter daily aerosol CONCsur over southern China in EL is consistently smaller than that in CLI bellow 70 μg m^{-3}, and generally larger than that in CLI above 70 μg m^{-3}, especially when aerosol CONCsur is larger than 130 μg m^{-3}. In other words, southern China tends to have less clean and heavy haze days but more moderate haze days than normal in La Niña winter. Whereas, in El Niño winter, southern China tends to have more heavy haze days but less clean and moderate haze days than normal. This explains why southern China has less (more) haze days but more (less) atmospheric contents of aerosols than normal in El Niño (La Niña) winter.

It is depicted in Figure 11 that under the emission level of aerosols for the year 2010, the enhanced (weakened) transports of aerosols from South and Southeast Asia to southern China caused by El Niño (La Niña) is the main reason for the increase (decrease) in the atmospheric contents of aerosols over southern China in El Niño (La Niña) winter. Therefore, it is expected that when the emissions of aerosols over South and Southeast Asia diminish in the future, the contradiction between the influences of ENSO on the winter haze days and atmospheric contents of aerosols over southern China will also disappear.

4 Conclusions and discussions

The effects of ENSO on the winter haze days and atmospheric contents of aerosols over China are discussed statistically and numerically. Statistical results show that southern China tends to have less (more) haze days than normal in El Niño (La Niña) winter, which is in line with the simulated more (less) winter precipitation over southern China caused by El Niño (La Niña). Statistical results indicate that the winter haze days over northern and eastern China have no significant relationship with ENSO. Numerical results also reveal that the changes in the winter-average atmospheric contents of aerosols caused by El Niño and La Niña are not quite different with each other over northern and eastern China. As a tropical phenomenon, it seems that ENSO affects the winter haze pollution over southern China more significantly than elsewhere of the country. The result confirms that the influencing factors of the winter haze pollution over northern and eastern China are in the mid and high latitudes as many studies introduced in section 1 have already explored.

Numerical results indicate that the atmospheric contents of aerosols over southern China are more (less) than normal in El Niño (La Niña) winter, which is to some extent not in line with the effects of ENSO on the winter haze days of the region. In 2010, South and Southeast Asia have become important source areas of anthropogenic aerosols (Zhang et al., 2016). The enhanced southwesterly (northeasterly) at the northwest of the winter anomalous anticyclone (cyclone) over western North Pacific caused by El Niño (La Niña) enhanced (weakened) the transports of aerosols from South and Southeast Asia to southern China. The PDF of the simulated winter daily surface concentrations of aerosols over southern China indicates that the region tends to have more heavy (moderate) haze days, but less clean and moderate (heavy) haze days than normal in El Niño (La Niña) winter. But it should be noted again that the emission data of aerosols used in our study is fixed in 2010, and if the emissions of aerosols changed the story might be different.

Haze pollution is a very sophisticated problem, because it is the comprehensive result of human activities and weather conditions. Weather conditions determine the dispersions and removals of haze particles over a specific region, influence the complex chemistry reactions among different components, and also connect the haze pollution of a specific region with the emissions of neighboring regions. To be more complicated, haze pollution and weather conditions interact with each other closely over some areas. This work explores the effects of ENSO on the winter haze pollution over China under relative simple experimental settings, with prescribed SST and fixed aerosol emissions, which means that SST does not response to aerosols.

Besides, the chemistry reactions in the model we used is also simplified, especially without the complex reactions related to nitrate aerosols. Therefore, studies with more sophisticated experimental designs (e.g., with atmosphere and ocean coupled models) and chemistry schemes are still in need in the future as to the topic discussed in this work.

Author contributions. The work was done under the guidance of Hua Zhang. Shuyun Zhao and Hua Zhang designed the experiment, and prepared the manuscript. Bing Xie conducted model simulations. The analysis of results and preparation of all figures and tables were done by Shuyun Zhao.

Acknowledgement

This work was financially supported by the (Key) National Natural Science Foundation of China (91644211&41575002). And we would like to thank Dr. Shao Sun of the National Climate Center, Chinese Meteorological Administration, for his kind help in plotting figures.

References

Bjerknes, J.: Large-scale atmospheric response to the 1964-65 Pacific equatorial warming, J. Phys. Oceanogr., 2, 212–217, doi: 10.1175/1520-0485(1972)002<0212:LSARTT>2.0.CO;2, 1972.

Cao, J.-J., Lee, S.-C., Chow, J.-C., Watson, J. G., Ho, K.-F., Zhang, R.-J., Jin, Z.-D., Shen, Z.-X., Chen, G.-C., Kang, Y.-M., Zou, S.-C., Zhang, L.-Z., Qi, S.-H., Dai, M.-H., Cheng, Y., and Hu, K.: Spatial and seasonal distributions of carbonaceous aerosols over China, J. Geophys. Res., 112, D22S11, doi: 10.1029/2006JD008205, 2007.

Cai, W.-J., Li, K., Liao, H., Wang, H.-J., and Wu, L.-X.: Weather conditions conducive to Beijing severe haze more frequent under climate change, Nature Climate Change, Nat. Clim. Change, 7, 257–262, doi: 10.1038/nclimate3249, 2017.

Chang, C.-P., Zhang, Y.-S., and Li, T.: Interannual and interdecadal variations of the East Asian summer monsoon and tropical Pacific SSTs. Part I: Roles of the subtropical ridge, J. Climate, 13, 4310–4325, doi: 10.1175/1520-0442(2000)013<4310:IAIVOT>2.0.CO;2, 2000.

Chen, W., Graf, H. F., and Huang, R.-H.: The interannual variability of East Asian winter monsoon and its relation to the summer monsoon, Adv. Atmos. Sci., 17, 48–60, doi: 10.1007/s00376-000-0042-5, 2000.

Chen, W., Lan, X.-Q., Wang, L., and Ma, Y.: The combined effects of the ENSO and the Arctic Oscillation on the winter

climate anomalies in East Asia, Chin. Sci. Bull., 58(12), 1355–1362, doi: 10.1007/s11434-012-5654-5, 2013.

Chen, H.-P. and Wang, H.-J.: Haze days in North China and the associated atmospheric circulations based on daily visibility data from 1960 to 2012, J. Geophys. Res.: Atmos., 120 (12), 5895–5909, doi: 10.1002/2015JD023225, 2015.

Chin M.: Dirtier air from a weaker monsoon, Nature Geoscience, 5, 449–450, doi: 10.1038/ngeo1513, 2012.

Dawson, J. P., Adams, P. J., and Pandis, S. N.: Sensitivity of $PM_{2.5}$ to climate in the Eastern US: a modeling case study, Atmos. Chem. Phys., 7, 4295–4309, doi: 10.5194/acp-7-4295-2007, 2007.

Ding, Y.-H. and Liu, Y.-J.: Analysis of long-term variations of fog and haze in China in recent 50 years and their relations with atmospheric humidity, Sci. China Earth Sci., 57, 36–46, doi: 10.1007/s11430-013-4792-1, 2014.

Feng, J., Li, J.-P., Zhu, J.-L., and Liao, H.: Influences of El Nino Modoki event 1994/1995 on aerosol concentrations over southern China, J. Geophys. Res: Atmos., 121(4), 1637–1651, doi: 10.1002/2015JD023659, 2016.

Gao, H. and Li, X.: Influences of El Nino Southern Oscillation events on haze frequency in eastern China during boreal winters, Int. J. Climatol., 35(9), 2682–2688, doi: 10.1002/joc.4133, 2015.

Gong, S.-L., Barrie, L. A., and Lazare, M.: Canadian Aerosol Module (CAM): a size-segregated simulation of atmospheric aerosol processes for climate and air quality models 2. Global sea-salt aerosol and its budgets, J. Geophys. Res., 107(D24), doi: 10.1029/2001JD002004, 2002.

Gong, S.-L., Barrie, L. A., Blanchet, J.-P., von Salzen, K., Lohmann, U., Lesins, G., Spacek, L., Zhang, L.-M., Girard, E., Lin, H., Leaitch, R., Leighton, H., Chylek, P., and Huang, P.: Canadian aerosol module: A size-segregated simulation of atmospheric aerosol processes for climate and air quality models 1. Module development, J. Geophys. Res., 108(D1), doi: 10.1029/2001JD002002, 2003.

He, S.-P. and Wang, H.-J.: Oscillating relationship between the East Asia winter monsoon and ENSO, J. Climate, 26, 9819–9838, doi: 10.1175/JCLI-D-13-00174.1, 2013.

Huang, R.-H. and Wu, Y.-F.: The influence of ENSO on the summer climate change in China and its mechanism, Adv. Atmos. Sci., 6 (1), 21–32, doi: 10.1007/BF02656915, 1989.

Huang, R.-H., Chen, J.-L., Wang, L., and Lin, Z.-D.: Characteristics, processes, and causes of the spatio-temporal variabilities of the East Asian monsoon system, Adv. Atmos. Sci., 29, 910–942, doi: 10.1007/s00376-012-2015-x, 2012.

Hurrell, J. W., Hack, J. J., Shea, D., Caron, J. M., and Rosinski, J.: A new sea surface temperature and sea ice boundary data set for the Community Atmosphere Model, J. Climate, 21, 5145–5153, doi: 10.1175/2008JCLI2292.1, 2008.

Jacob, D. J. and Winner, D. A.: Effects of climate change on air quality, Atmos. Environ., 43, 51–63, doi: 10.1016/j.atmosenv.2008.09.051, 2009.

Kim, J.-W., An, S.-I., Jun, S.-Y., Park, H.-J., and Yeh, S.-W.: ENSO and East Asian winter monsoon relationship modulation associated with the anomalous northwest Pacific anticyclone, Clim. Dyn., doi: 10.1007/s00382-016-3371-5, 2016.

Lau, N.-C. and Nath, M. J.: Atmosphere-ocean variations in the Indo-Pacific sector during ENSO episodes, J. Climate, 16, 3–20, doi: 10.1175/1520-0442(2003)016<0003:AOVITI>2.0.CO;2, 2003.

Li, Q., Zhang, R.-H., and Wang, Y.: Interannual variation of the wintertime fog-haze days across central and eastern China and its relation with East Asian winter monsoon, Int. J. Climatol., 36, 346–354, doi: 10.1002/joc.4350, 2016a.

Li, Y., Lu, R.-Y., and Dong, B.-W.: The ENSO-Asian monsoon interaction in a coupled ocean-atmosphere GCM, J. Climate, 20, 5164–5177, doi: 10.1175/JCLI4289.1, 2007.

Li, Z.-Q., Lau, W. K.-M., Ramanathan, V., Wu, G., Ding, Y., Manoj, M.-G., Liu, J., Qian, Y., Li, J., Zhou, T., Fan, J., Rosenfeld, D., Ming, Y., Wang, Y., Huang, J., Wang, B., Xu, X., Lee, S.-S., Cribb, M., Zhang, F., Yang, X., Zhao, C., Takemura, T., Wang, K., Xia, X., Yin, Y., Zhang, H., Guo, J., Zhai, P.-M., Sugimoto, N., Babu, S.-S., and Brasseur G.-P.: Aerosol and monsoon climate interactions over Asia, Rew. Geophys., 54, 866–929, doi: 10.1002/2015RG000500, 2016b.

Liu, X.-D., Yan, L.-B., Yang, P., Yin, Z.-Y., and North, G. R.: Influence of Indian summer monsoon on aerosol loading in East Asia, J. Appl. Meteor. Climatol., 50, 523–533, doi: 10.1175/2010JAMC2414.1, 2011.

Mu, M. and Zhang, R.-H.: Addressing the issue of fog and haze: A promising perspective from meteorological science and technology, Sci. China Earth Sci., 57, 1–2, doi: 10.1007/s11430-013-4791-2, 2014.

Rasmusson, E. M. and Carpenter, T. H.: Variations in tropical sea surface temperature and surface wind fields associated with the Southern Oscillation/El Niño, Mon. Wea. Rev., 110, 354–384, doi: 10.1175/1520-0493(1982)110<0354:VITSST>2.0.CO;2, 1982.

Tao, M.-H., Chen, L.-F., Xiong, X.-Z., Zhang, M.-G., Ma, P.-F., Tao, J.-H., and Wang, Z.-F.: Formation process of the widespread extreme haze pollution over northern China in January 2013: Implications for regional air quality and climate,

Atmos. Environ., 98, 417–425, doi: 10.1016/j.atmosenv.2014.09.026, 2014.

Tao, M.-H., Chen, L.-F., Wang, Z.-F., Wang, J., Tao, J.-H., and Wang, X.-H.: Did the widespread haze pollution over China increase during the last decade? A satellite view from space, Environ. Res. Lett., 11(5),054019, doi: 10.1088/1748-9326/11/5/054019, 2016.

Wang, B., Wu, R.-G., and Fu, X.-H.: Pacific-East Asian Teleconnection: How does ENSO affect East Asian Climate? J. Climate, 13, 1517–1536, doi: 10.1175/1520-0442(2000)013<1517:PEATHD>2.0.CO;2, 2000.

Wang, H.-J., Chen, H.-P., and Liu, J.-P.: Arctic sea ice decline intensified haze pollution in eastern China, Atmos., Oceanic Sci. Lett., 8, 1–9, doi: 10.3878/AOSL20140081, 2015.

Wang. L. and Chen, W.: An intensity index for the East Asian winter monsoon, J. Climate, 27, 2361–2374, doi: 10.1175/JCLI-D-13-00086.1, 2014.

Wang, Y.-S., Yao, L., Wang, L.-L., Liu, Z.-R., Ji, D.-S., Tang, G.-Q., Zhang, J.-K., Sun, Y., Hu, B., and Xin, J.-Y.: Mechanism for the formation of the January 2013 heavy haze pollution episode over central and eastern China, Sci. China Earth Sci., 57, 14–25, doi: 10.1007/s11430-013-4773-4, 2014a.

Wang, Z.-F., Li, J., Wang, Z., Yang, W.-Y., Tang, X., Ge, B.-Z., Yan, P.-Z., Zhu, L.-L., Chen, X.-S., Chen, H.-S., Wand, W., Li, J.-J., Liu, B., Wang, X.-Y., Wand, W., Zhao, Y.-L., Lu, N., and Su, D.-B.: Modeling study of regional severe hazes over mid-eastern China in January 2013 and its implications on pollution prevention and control, Sci. China Earth Sci., 57, 3–13, doi: 10.1007/s11430-013-4793-0, 2014b.

Wang, Z.-L., Zhang, H., and Zhang, X.-Y.: Projected responses of East Asian summer monsoon system to future reductions in emissions of anthropogenic aerosols and their precursors, Clim. Dyn., 47(5), 1455–1468, doi: 10.1007/s00382-015-2912-7, 2015.

Wu, T.-W., Yu, R.-C., Zhang, F., Wang, Z.-Z., Dong, M., Wang, L.-N., Jin, X., Chen, D.-L., and Li, L.: The Beijing Climate Center atmospheric general circulation model: description and its performance for the present-day climate, Clim. Dyn., 34, 123–147, doi: 10.1007/s00382-008-0487-2, 2010.

Yan, L.-P., Liu, X.-D., Yang, P., Yin, Z.-Y., and North, G. R.: Study of the impact of summer monsoon circulation on spatial distribution of aerosols in East Asia based on numerical simulation, J. Appl. Meteor. Climatol., 50, 2270–2282, doi:

10.1175/2011JAMC-D-11-06.1, 2011.

Zhai, P.-M., Yu, R., Guo, Y.-J., Li, Q.-X., Ren, X.-J., Wang, Y.-Q., Xu, W.-H., Liu, Y.-J., and Ding, Y.-H.: The strong El Niño of 2015/16 and its dominant impacts on global and China's climate, J. Meteor. Res., 30(3), 283–297, doi: 10.1007/s13351-016-6101-3, 2016.

Zhang, H., Wang, Z.-L., Wang, Z.-Z., Liu, Q.-X., Gong, S.-L., Zhang, X.-Y., Shen, Z.-P., Lu, P., Wei, X.-D., Che, H.-Z., and Li, L.: Simulation of direct radiative forcing of aerosols and their effects on East Asia climate using an interactive AGCM-aerosol coupled system, Clim. Dyn., 38, 1675–1693, doi: 10.1007/s00382-011-1131-0, 2012.

Zhang, H., Zhao, S.-Y., Wang, Z.-L., Zhang, X.-Y., and Song, L.-C.: The updated effective radiative forcing of major anthropogenic aerosols and their effects on global climate at present and in the future, Int. J. Climatol., 36(12), 4029–4044, doi: 10.1002/joc.4613, 2016.

Zhang, L., Liao, H., and Li, J.-P.: Impacts of Asian summer monsoon on seasonal and interannual variations of aerosols over eastern China, J. Geophys. Res., 115, D716, doi: 10.1029/2009JD012299, 2010.

Zhang, R.-H., Sumi, A., and Kimoto, M.: A diagnostic study of the impact of El Niño on the precipitation in China, Adv. Atmos. Sci., 16(2), 229–241, doi: 10.1007/BF02973084, 1999.

Zhang, R.-H., Li, Q., and Zhang, R.-N.: Meteorological conditions for the persistent severe fog and haze event over eastern China in January 2013, Sci. China Earth Sci., 57, 26–35, doi: 10.1007/s11430-013-4774-3, 2014.

Zhang, X.-Y., Wang, Y.-Q., Niu, T., Zhang, X.-C., Gong, S.-L., Zhang, Y.-M., and Sun, J.-Y.: Atmospheric aerosol compositions in China: spatial/temporal variability, chemical signature, regional haze distribution and comparisons with global aerosols, Atmos. Chem. Phys., 12, 779–799, doi: 10.5194/acp-12-779-2012, 2012.

Zhang, Y.-L. and Cao, F.: Fine particulate matter ($PM_{2.5}$) in China at a city level, Scientific Reports, 5, 14884, doi: 10.1038/srep14884, 2015.

Zhao, S.-Y., Zhi, X.-F., Zhang, H., Wang, Z.-L., and Wang, Z.-Z.: Primary assessment of the simulated climatic state using a coupled aerosol-climate model BCC_AGCM2.0.1_CAM. Climatic and Environmental Research (in Chinese), 19(3), 265–277, doi: 10.3878/j.issn.1006-9585.2012.12015, 2014.

Zhao, S.-Y., Chen, L.-J., and Cui, T.: Effects of ENSO phase-switching on rainy-season precipitation in north China, Chinese

Journal of Atmospheric Sciences (in Chinese), doi: 10.3878/j.issn.1006-9895.1701.16226, 2017.

Zhu, J.-L., Liao, H., and Li J.-P.: Increases in aerosol concentrations over eastern China due to the decadal-scale weakening of the East Asian summer monsoon, Geophys. Res. Lett., 39, L09809, doi: 10.1029/2012GL051428, 2012.

Zou, Y.-F., Wang, Y.-H., Zhang, Y.-Z., and Koo, J.-H.: Arctic sea ice, Eurasia snow, and extreme winter haze in China, Sci. Adv., 3, e1602751, doi: 10.1126/sciadv.1602751, 2017.

Tables and Figures

Table 1. Simulation set-up.

Group name	SST	Running time	Output frequency
CLI	Climatologic SST	Oct.^{0}–Aug.^{1}	Monthly & Daily
EL	Climatologic SST + $\Delta SST_{El\ Niño}$	Oct.^{0}–Feb.^{1}	Monthly & Daily
LA	Climatologic SST + $\Delta SST_{La\ Niña}$	Oct.^{0}–Feb.^{1}	Monthly & Daily

The superscripts of the 3rd column: 0 and 1 represent the 1st and 2nd model year, respectively.

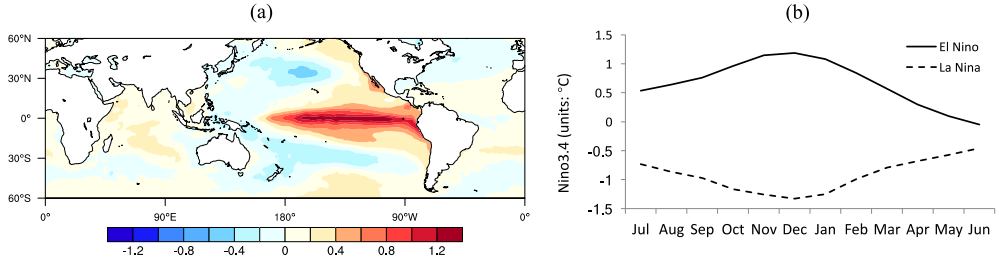

Figure 1. (a) Typical ENSO mode (units: °C/°C) and (b) average monthly Niño3.4 (units: °C) of 21 El Niño and 18 La Niña events from 1951 to 2015.

Atmos. Chem. Phys. Discuss., https://doi.org/10.5194/acp-2017-506
Manuscript under review for journal Atmos. Chem. Phys.
Discussion started: 22 June 2017

Atmospheric Chemistry and Physics Discussions

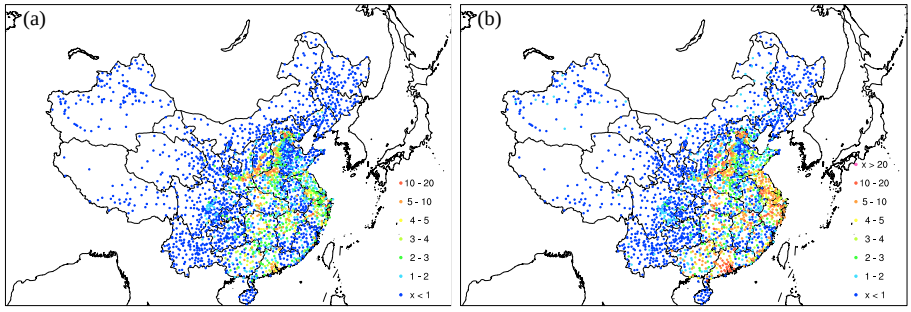

Figure 2. The winter-average monthly haze days (units: days/month) during the years of (a) 1960-2013 and (b) 2000-2013 over main land China.

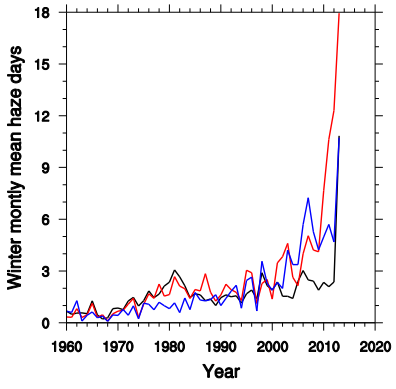

Figure 3. Time series of the winter-average monthly haze days (units: days/month) of JJJ (black), JZH (red), and GG (blue).

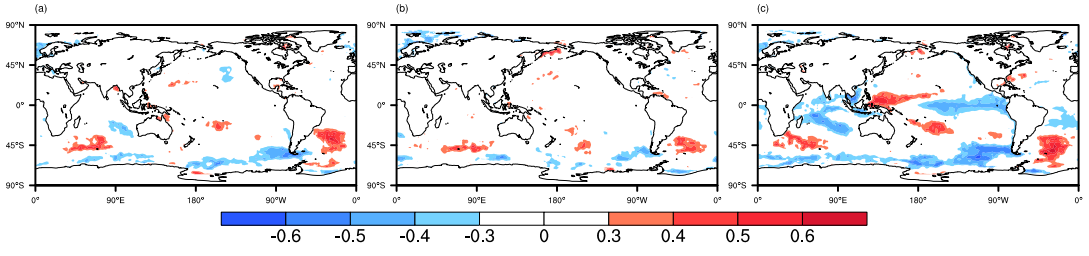

Figure 4. Correlation coefficients (unitless) of the monthly haze days of (a) JJJ, (b) JZH, and (c) GG with SST in winter, after applying a linear-trend removing and 2-8 years' band-pass filtering to both the data of haze days and SST. Shade denotes that results pass 95% significance level.

Atmos. Chem. Phys. Discuss., https://doi.org/10.5194/acp-2017-506
Manuscript under review for journal Atmos. Chem. Phys.
Discussion started: 22 June 2017

Atmospheric Chemistry and Physics Discussions

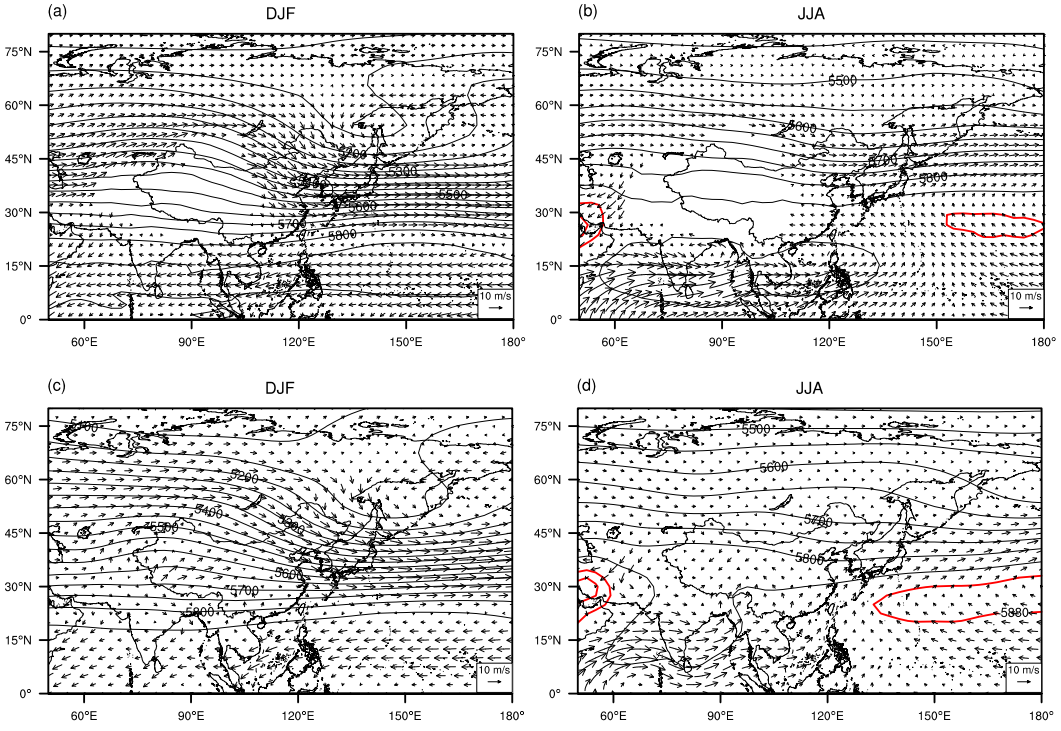

Figure 5. The simulated ensemble-mean (a) winter and (b) summer geopotential height (contour, units: gpm) at 500 hPa and wind field (vector, units: m s^{-1}) at 850 hPa in the group of CLI; (c) and (d) are the same with (a) and (b), but data are from NCEP reanalysis data.

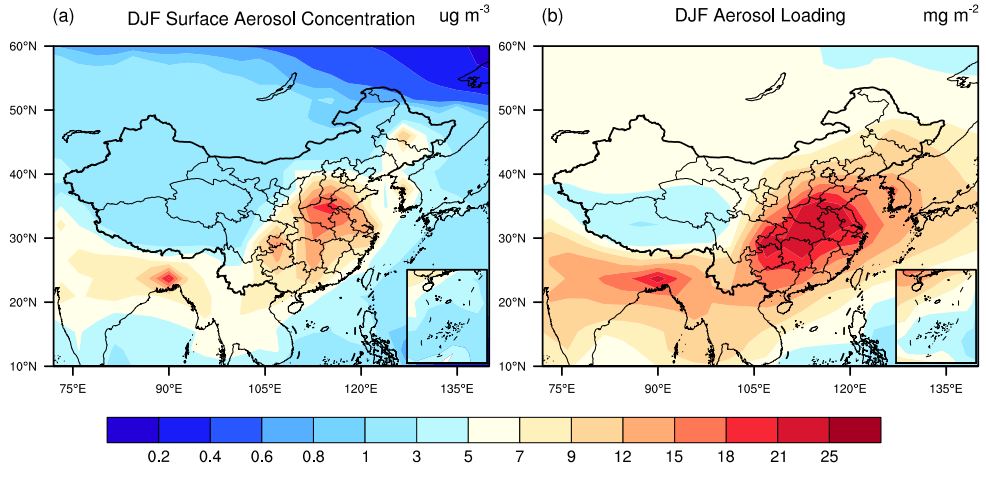

Figure 6. The simulated winter-average (a) surface aerosol concentrations (units: μg m^{-3}) and (b) aerosol loadings (units: mg m^{-2}) in

Atmos. Chem. Phys. Discuss., https://doi.org/10.5194/acp-2017-506
Manuscript under review for journal Atmos. Chem. Phys.
Discussion started: 22 June 2017

Atmospheric Chemistry and Physics Discussions

the group of CLI.

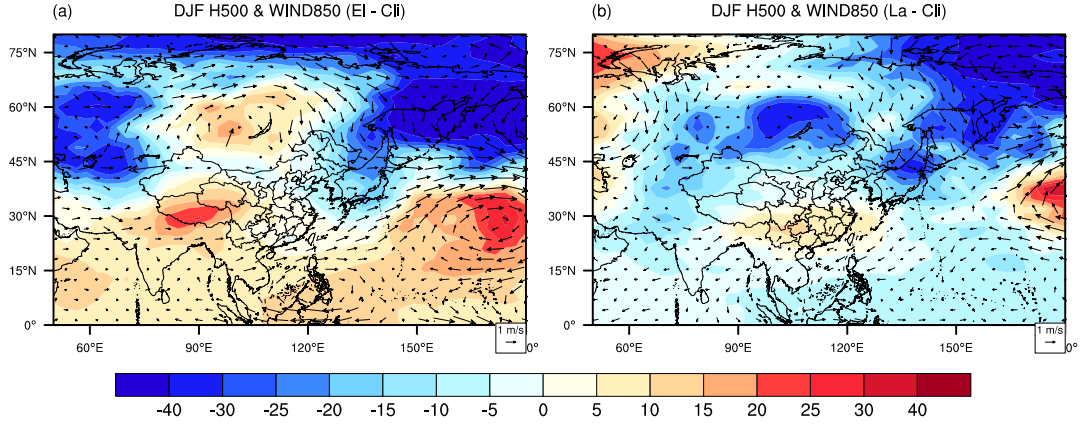

Figure 7. Medians of the simulated changes in winter-average geopotential height (counters, units: gpm) at 500 hPa and wind (vectors, units: m s^{-1}) at 850 hPa, caused by (a) El Niño and (b) La Niña.

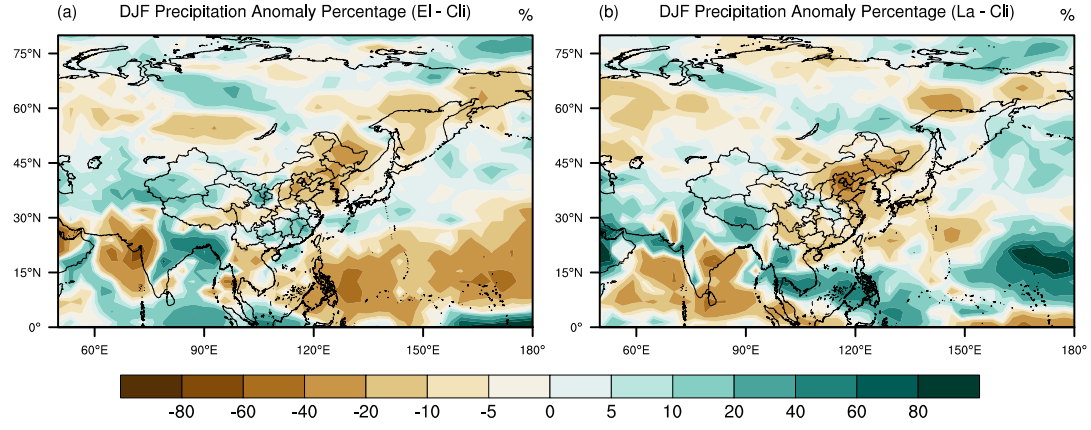

Figure 8. Medians of the simulated changes in winter-average precipitation in percentage (units: %) caused by (a) El Niño and (b) La Niña.

Atmos. Chem. Phys. Discuss., https://doi.org/10.5194/acp-2017-506
Manuscript under review for journal Atmos. Chem. Phys.
Discussion started: 22 June 2017

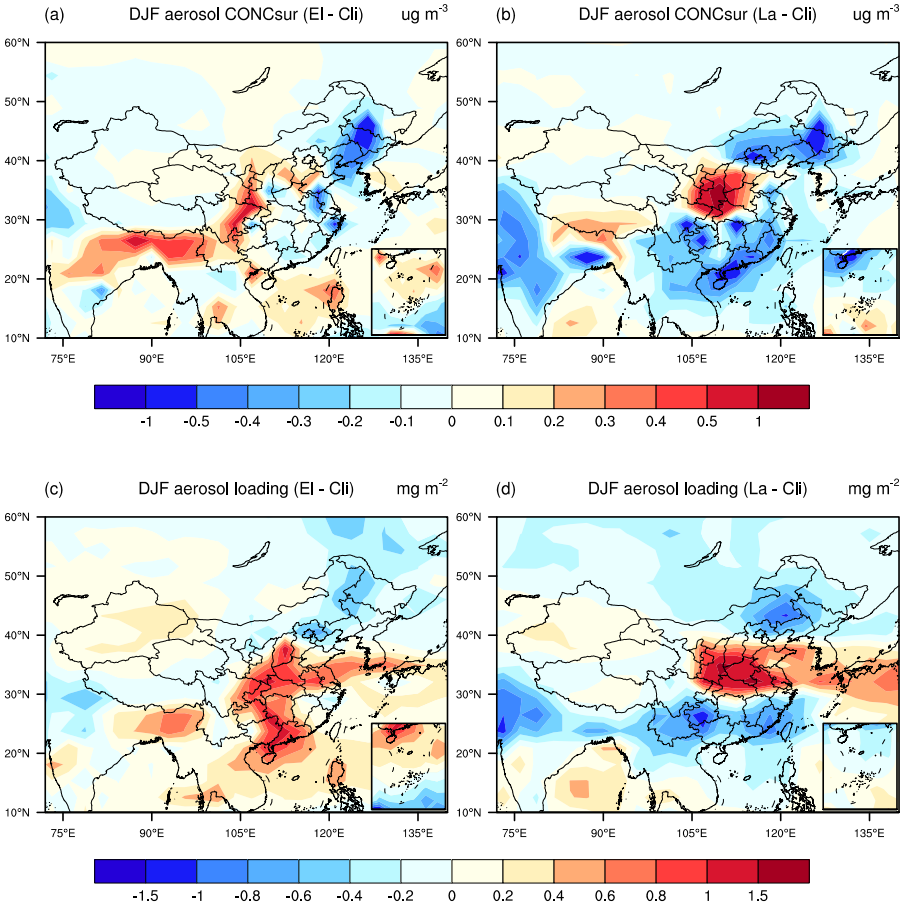

Figure 9. Medians of the simulated changes in winter-average aerosol surface concentrations (units: μg m^{-3}) caused by (a) El and (b) La; (c) and (d) are the same with (a) and (b), but for the aerosol loadings (units: mg m^{-2}).

Atmos. Chem. Phys. Discuss., https://doi.org/10.5194/acp-2017-506
Manuscript under review for journal Atmos. Chem. Phys.
Discussion started: 22 June 2017

Atmospheric Chemistry and Physics Discussions

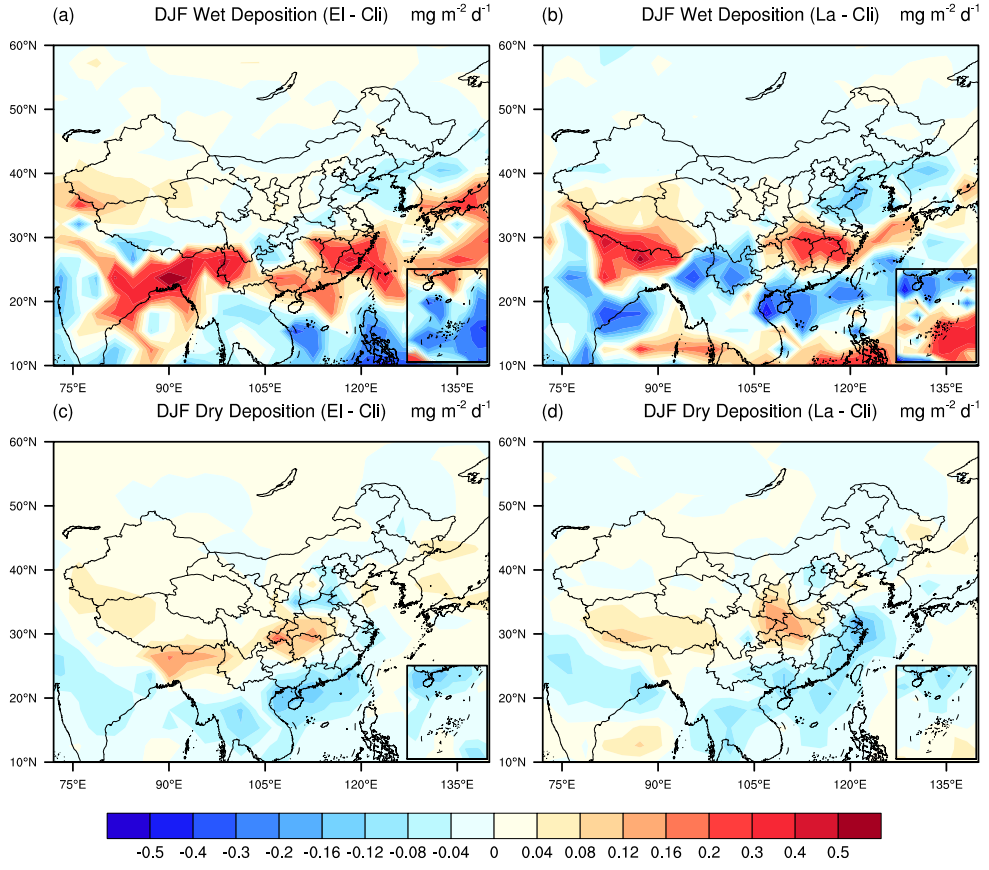

Figure 10. Medians of the simulated changes in winter-average wet depositions (units: mg m^{-2} d^{-1}) of aerosols caused by (a) El Niño, and (b) La Niña; (c) and (d) are the same with (a) and (b), but for the dry depositions of aerosols.

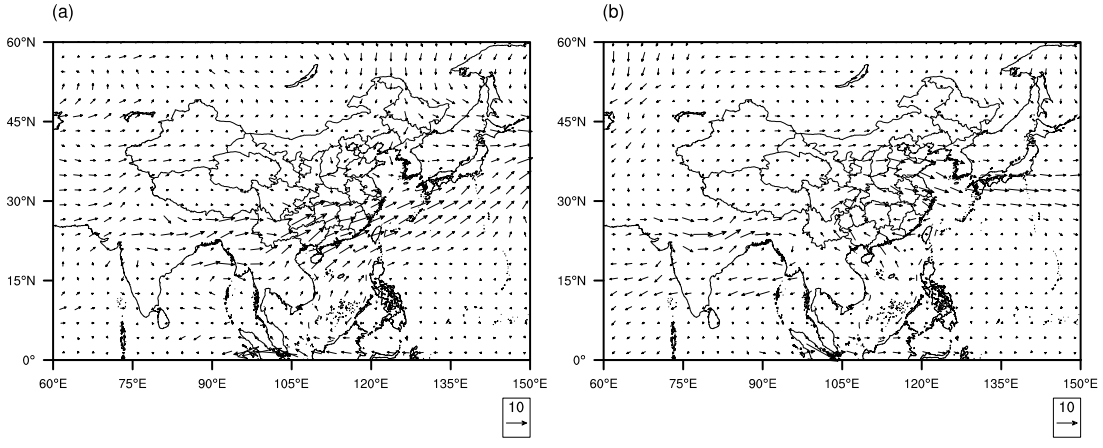

Atmos. Chem. Phys. Discuss., https://doi.org/10.5194/acp-2017-506
Manuscript under review for journal Atmos. Chem. Phys.
Discussion started: 22 June 2017

Atmospheric Chemistry and Physics Discussions

Figure 11. Medians of the simulated changes in winter-average vertical integral of aerosol zonal flux (units: kg $m^{-1}s^{-1}$) caused by (a) El Niño, and (b) La Niña.

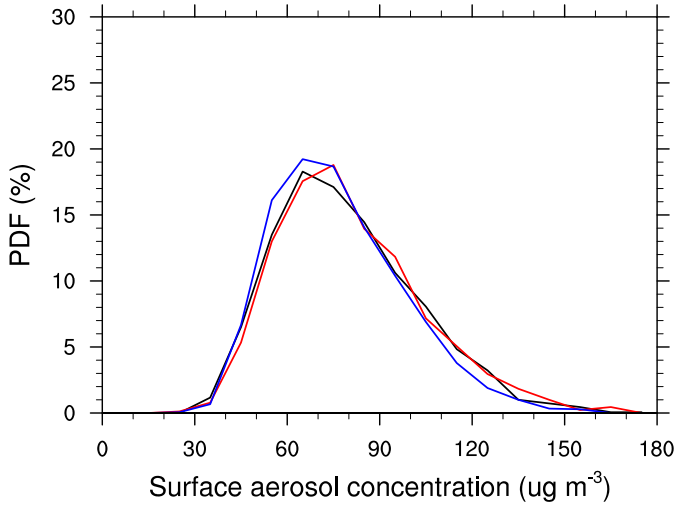

Figure 12. Probability distribution of the simulated winter daily surface aerosol concentration averaged over southern China (after being amplified by 10 times); Black, red and blue lines represent the results from experiment groups of CLI, EL, and LA, respectively.